ISSCR

Environmental Elasticity Regulates Cell-type Specific RHOA Signaling and Neuritogenesis of Human Neurons

Robert H. Nichol IV,[1,2] Timothy S. Catlett,[1,3] Massimo M. Onesto,[1] Drew Hollender,[1] and Timothy M. Gómez[1,2,3,*]

[1]Department of Neuroscience, University of Wisconsin School of Medicine and Public Health, WIMR II Room 5433, 1111 Highland Avenue, Madison, WI 53706, USA
[2]Neuroscience Training Program, University of Wisconsin School of Medicine and Public Health, WIMR II Room 5433, 1111 Highland Avenue, Madison, WI 53706, USA
[3]Graduate Program in Cellular and Molecular Biology, University of Wisconsin School of Medicine and Public Health, WIMR II Room 5433, 1111 Highland Avenue, Madison, WI 53706, USA
*Correspondence: tmgomez@wisc.edu
https://doi.org/10.1016/j.stemcr.2019.10.008

SUMMARY

The microenvironment of developing neurons is a dynamic landscape of both chemical and mechanical cues that regulate cell proliferation, differentiation, migration, and axon extension. While the regulatory roles of chemical ligands in neuronal morphogenesis have been described, little is known about how mechanical forces influence neurite development. Here, we tested how substratum elasticity regulates neurite development of human forebrain (hFB) neurons and human motor neurons (hMNs), two populations of neurons that naturally extend axons into distinct elastic environments. Using polyacrylamide and collagen hydrogels of varying compliance, we find that hMNs preferred rigid conditions that approximate the elasticity of muscle, whereas hFB neurons preferred softer conditions that approximate brain tissue elasticity. More stable leading-edge protrusions, increased peripheral adhesions, and elevated RHOA signaling of hMN growth cones contributed to faster neurite outgrowth on rigid substrata. Our data suggest that RHOA balances contractile and adhesive forces in response to substratum elasticity.

INTRODUCTION

Neuronal growth cones are sensorimotor terminals of developing axons that use local cues in their environment to guide process extension. The study of axon guidance has largely focused on how soluble chemical ligands, released into the local extracellular environment near choice points, induce morphological changes within growth cones to regulate the rate and direction of outgrowth (Lowery and Van Vactor, 2009; Tessier-Lavigne and Goodman, 1996). However, research indicates that most secreted guidance cues and growth factors are likely immobilized to the extracellular matrix (ECM) or cell surface *in vivo*. For example, chemotropic guidance toward netrin depends on ligand immobilization to the substratum (Moore et al., 2010, 2012). Other secreted factors, such as neurotrophins, bone morphogenic proteins, Slits, and Semaphorins, also bind to ECM proteins, which suggests similar immobilization-dependent signaling (De Wit et al., 2005; Hu, 2001; Hynes, 2009; Kerstein et al., 2015). Interactions between ECM proteins, growth factors, and cell-surface receptors indicate that many ligands serve as both adhesive contacts and activators of intracellular signals. While increasing evidence suggests that growth cones respond to adhesion-dependent mechanical signals (Kerstein et al., 2015; Gomez et al., 1996; Kerstein et al., 2017; Kostic et al., 2007), the precise role of environment elasticity on neurite extension and guidance is still poorly understood.

During embryogenesis, neurons extend axons along and through tissues of widely varying elasticities en route to their central and peripheral target sites. Elasticity is measured as the deformability of a material in response to mechanical force and is represented as the Young's modulus or elastic modulus (measured in pascals [Pa]). Using magnetic resonance elastography, human tissue elasticity was found to vary widely within and between tissues, including brain, spinal cord, and peripheral tissues (Kruse et al., 2008; McCracken et al., 2005; Tyler, 2012). In fact, regions of the central nervous system (CNS) in both human and rodent appear to have elastic moduli ranging from 0.1 kPa to 16 kPa (Tyler, 2012). Therefore, axonal projections within the CNS traverse a range of relatively soft elastic conditions (Franze, 2013; Koser et al., 2016). However, some projection neurons, such as motor neurons (MNs) and dorsal root ganglion (DRG) neurons, project axons both within soft CNS environments and across more rigid peripheral tissues. Peripheral tissues, such as connective tissue and arteries (0.1–1 MPa), muscle (10–100 kPa), and bone (15–30 GPa), are significantly more rigid than the CNS (Franze, 2013; Tyler, 2012). Therefore, MN axonal projections provide an interesting model to examine elasticity-dependent axon extension, as MN axons initiate in soft CNS but subsequently exit the spinal cord through the dense meshwork of the basal lamina (Bonanomi and Pfaff, 2010).

Here, we used human MNs (hMNs) and human forebrain (hFB) neurons, differentiated from induced
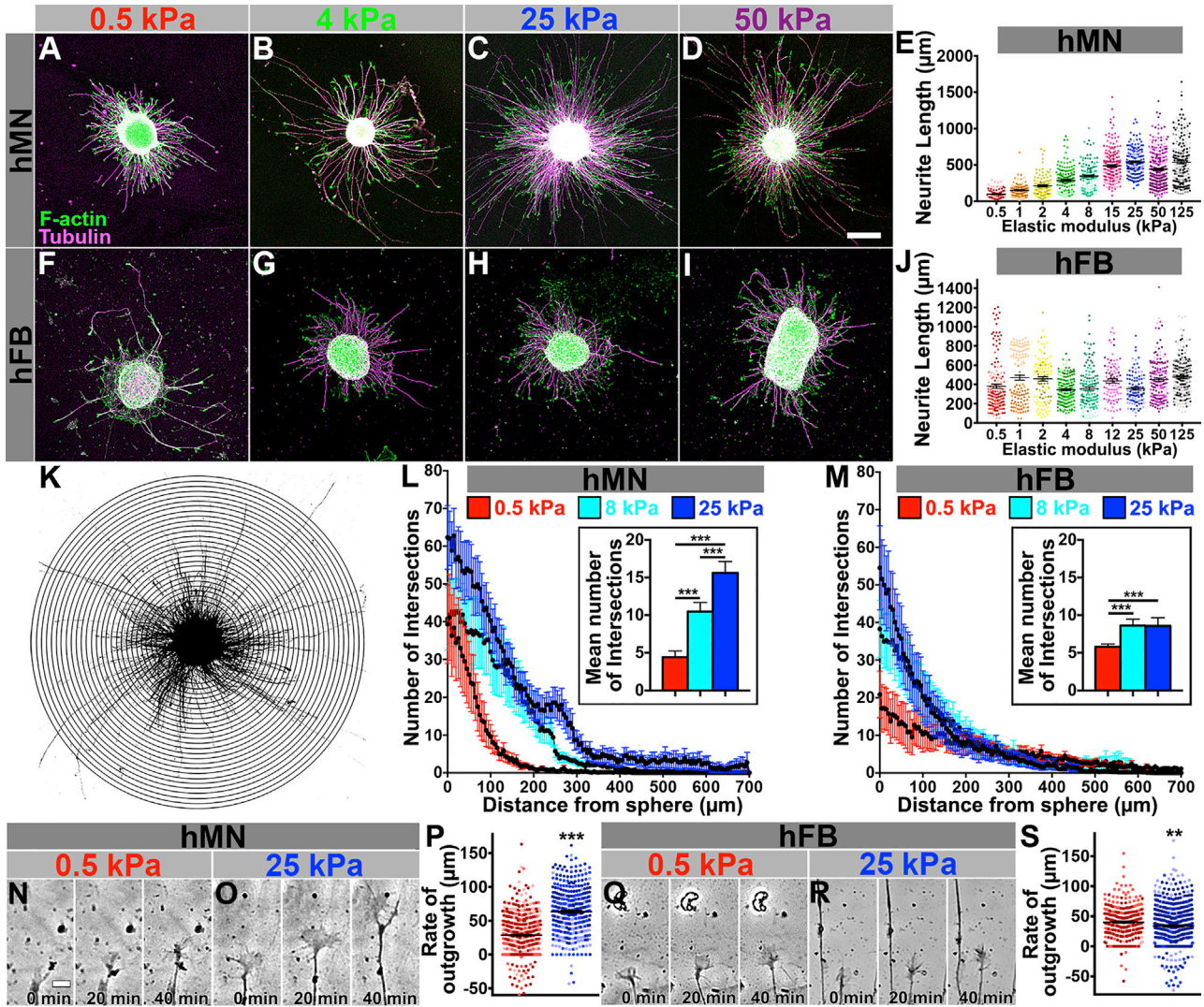
Figure 1. Substrata Elasticity Influences Neuronal Morphogenesis in a Neuronal-type Specific Manner in Two-Dimensional Cultures

(A–D) Low-magnification confocal images of iPSC-derived hMN neurospheres cultured on soft (0.5 kPa), intermediate (4 kPa), and rigid (25 kPa and 50 kPa) LN-coated PAA gels, and immunolabeled for acetylated tubulin (magenta) and F-actin (phalloidin, green). Note longer processes on rigid substrata compared with soft and intermediate.

(E) hMN neurite lengths were measured on increasing PAA gel rigidities (0.5–125 kPa). Due to the density of neurites extending from neurospheres, the ten longest neurites were measured for this analysis and compared between experimental groups. hMNs extend greater neurite lengths on progressively more rigid substrata up to 25 kPa and fitted linear regression lines showed strong goodness of fit ($R^2 = 0.8952$) and are significantly more sloped ($p < 0.001$) compared with hFB neurons (below). $n \geq 40$ neurites from $n = 4$ experiments from $n = 2$ differentiations for each condition.

(F–I) Representative images of hFB neurospheres cultured on soft (0.5 kPa), intermediate (4 kPa), and rigid (25 kPa and 50 kPa) LN-coated PAA gels, and immunolabeled for acetylated tubulin (magenta) and F-actin (phalloidin, green). Note similar neurite lengths on each elastic condition.

(J) Quantification of the ten longest hFB neurite lengths on increasing PAA gel rigidities shows no significant trend across rigidities, and linear regression shows poor goodness of fit ($R^2 = 0.03432$). $n \geq 50$ neurites from $n = 4$ experiments from $n = 2$ differentiations for each condition.

(K) Inverted contrast grayscale image of a representative labeled neurosphere used for Sholl analysis (ImageJ plugin, see Experimental Procedures) to measure neurite number and length.

(L and M) Sholl analysis of all neurites confirms that there are more intersecting neurites at greater distances on more rigid substrata for hMNs (L), while hFB neurite lengths show a modest increased number of short processes on rigid substrata (M). Insets compare the mean

(legend continued on next page)

pluripotent stem cells (iPSCs), to examine the effects of substrata elasticity on neuritogenesis by these distinct classes of neurons. We show that hMNs generate longer neurites and extend faster on more rigid two-dimensional (2D) polyacrylamide (PAA) hydrogels and within more rigid three-dimensional (3D) collagen I hydrogels. In contrast, the rate of hFB neurite outgrowth was significantly faster on soft 2D substrata, and hFB neurons have longer processes in soft 3D collagen gels. Increased axon extension by hMNs on rigid substrata may be due to stronger adhesion, as indicated by more stable leading-edge protrusions. Consistent with increased adhesion, hMNs have elevated Ras homolog gene family member A (RHOA)-guanosine triphosphatase (GTPase) and myosin II activity on rigid substrata, suggesting that RHOA signaling may feedforward to promote contractility-dependent adhesion formation. Acute pharmacological manipulations of RHOA suggest that a balance of contractile motor and adhesive forces supports maximal growth of hMN neurites on rigid substrata. Finally, several mechanosensitive adhesion proteins are activated in hMNs on rigid substrata, which is dependent on optimal RHOA activity. These data illustrate an important role for RHOA signaling and adhesion in regulating environmental elasticity-dependent development of class-specific human neurons.

RESULTS

Substrata Elasticity Determines Neurite Extension by Human Neurons in Two Dimensions

To test whether neurite development by central versus peripheral projecting human neurons is influenced by the mechanical environment, we cultured hMNs and hFB neurons on PAA hydrogels coated with poly-D-lysine (PDL) and laminin (LN) ranging from 0.2 kPa to 125 kPa. PAA hydrogels of precise elastic moduli (Matrigen) are functionalized so that they bind ECM protein equivalently at all elasticities, which we confirmed with LN labeling (Figure S1). Specific classes of human neurons were generated using chemically defined culture conditions, as described previously (Doers et al., 2014; Du et al., 2015; Hu et al., 2010). Primitive neuroepithelial cells with rostral phenotypes were confirmed by expression of the anterior transcription factor PAX6 by day 15 of differentiation and FOXG1, a telencephalic transcription factor, was in most βIII-tubulin-positive hFB neurons (Figure S2). Conversely, spinal hMN cell fate was verified by expression of Islet1 (ISL1), a transcription factor associated with MN development. The majority of the βIII-tubulin-positive neurons co-labeled with ISL1 (Figure S2).

While hMN and hFB neurospheres adhere poorly to the softest substratum (0.2 kPa), possibly due to poor LN binding (not shown), neurites were present after 1–2 days in vitro (DIV) on all other LN-coated PAA hydrogels. Quantifying the longest isolated processes (see Experimental Procedures), we found that hMNs extend longer neurites across increasingly rigid substrata (Figures 1A–1E), reaching peak lengths at 25 kPa (Figures 1C and 1E). Note that these effects did not require an ECM as a substratum, as hMN neurospheres cultured on soft and stiff PDL-only coated PAA also showed length differences (Figure S3). Importantly, these are physiologically relevant elastic conditions encountered by MNs that extend into peripheral tissues. Sholl analysis (Figure 1K) of all neurites confirmed our measurements of longest neurites and showed increased numbers of processes on rigid substrata (Figure 1L). The high density of processes emerging from neurospheres on rigid substrata suggests that rigidity could have an effect on neurite initiation (Figure 1L). In contrast to hMNs, elasticity did not produce a consistent effect on neurite length of hFB neurons over the same elastic range on PAA-LN (Figures 1F–1J) or fibronectin (Figure S4). However, while hFB neurite lengths were not significantly affected by elasticities above 500 Pa, Sholl analysis shows that more rigid conditions promoted hFB neurite initiation (Figure 1M). These data are in accordance with previous findings showing no preferential outgrowth by hippocampal neurons over a similar elastic range (Koch et al., 2012).

Since the mechanical environment influences neuronal differentiation (Musah et al., 2014) and

number of total intersections, showing significant elasticity-dependent differences. n ≥ 13 neurons from n = 3 experiments from n = 2 differentiations for each condition. ***p < 0.001, one-way ANOVA. It should be noted that elasticity differences in hFB neurite extension are limited to short processes, suggesting possible effects on neurite initiation.

(N and O) Representative live-cell images over a 40-min time period of hMN neurites extending from neurospheres plated on soft and rigid PAA gels.

(P) Quantification of rate of outgrowth from time-lapse movies confirms that neurite extension from hMNs is significantly faster on rigid substrata. n ≥ 362 neurites from n = 3 experiments from n = 2 differentiations for each condition. ***p < 0.001, Student's t test.

(Q and R) Representative live-cell images over a 40-min time period of hFB neurites extending from neurospheres plated on soft and rigid PAA gels.

(S) Quantification of rate of outgrowth shows that neurite extension from hFB neurites is significantly faster on soft substrata. n ≥ 362 neurites from n = 3 experiments from n = 2 differentiations for each condition. **p < 0.01, Student's t test.

Scale bars in (D) and (N), 100 μm (apply also to A–I, N, O, Q, R). See also Figures S1–S4.
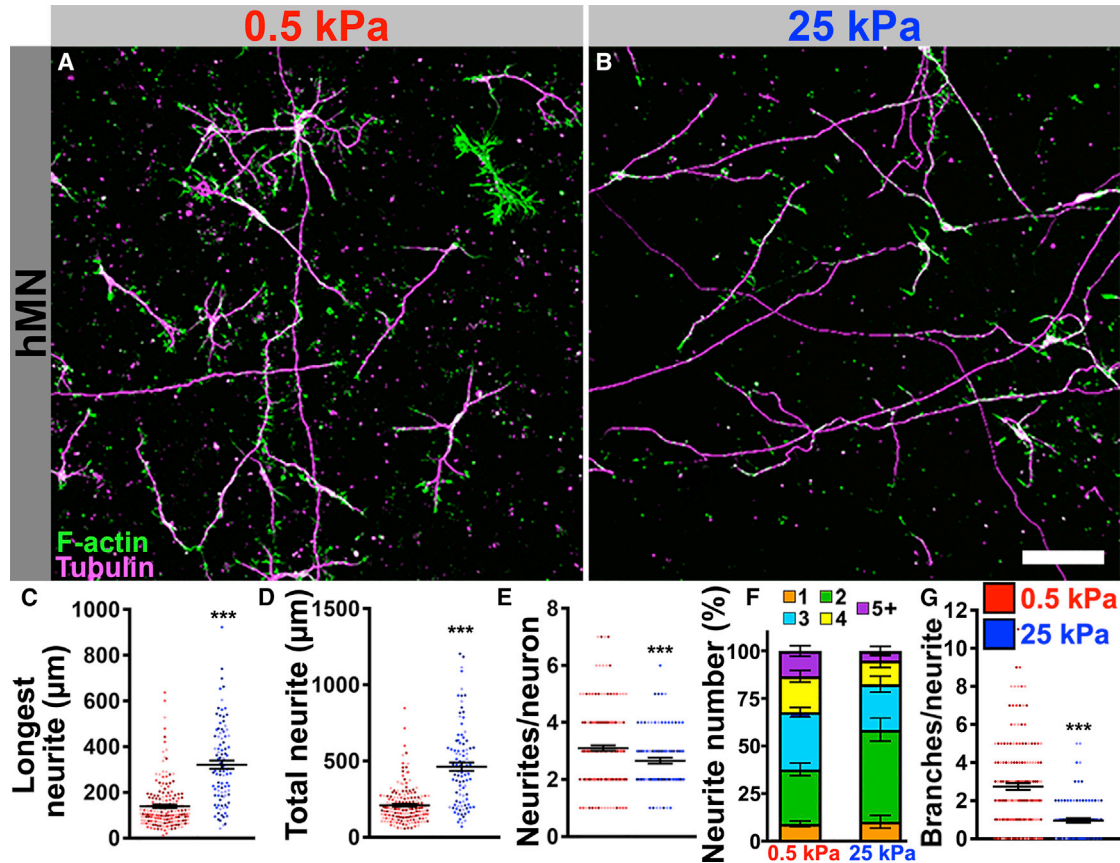
**Figure 2. Substrata Elasticity Influences Neuronal Morphogenesis in Dissociated Two-Dimensional Cultures**

(A and B) Dissociated hMNs on soft and rigid LN-coated PAA gels. Note that hMNs on 0.5 kPa (A) appear to have shorter, but more branched processes compared with 25 kPa (B).

(C–G) While the longest neurite (C) and total neurite length (D) of hMNs are greater on rigid substrata, the number of neurites per neuron are greater (E and F) and neurites are more branched (G) on soft substrata. n ≥ 96 neurites from n = 3 experiments from n = 2 differentiations for each condition. ***p < 0.001, Student's t test.

possibly process initiation, we asked whether substrata elasticity directly affected the rate of process extension. For this we quantified neurite outgrowth rates for hMNs and hFB neurons using live-cell imaging, again focusing on physiologically relevant 0.5- and 25-kPa conditions. Consistent with analysis of neurite lengths in fixed cell culture, the rates of hMN neurite outgrowth were significantly faster on rigid compared with soft substrata (Figures 1N–1P), suggesting that differential neurite lengths were due in part to differences in neurite extension rates. However, it should be noted that while the rate of neurite outgrowth was approximately two times faster on rigid substrata, hMN processes were nearly six times longer on rigid substrata after 2 days in culture, suggesting that rigid conditions may also accelerate neurite initiation. Time-lapse imaging of hFB neurons showed that neurite outgrowth was slightly slower on rigid compared with soft substrata (Figures 1Q–1S).

These results suggest that soft environments increase hFB neurite outgrowth rates, while rigid environments induce greater neurite number, as observed in Figure 1M, resulting in a similar number of long projecting neurites by hFB. These findings confirm the hypothesis that central and peripheral neurite extension rate is influenced by environmental elasticity.

To examine elasticity-dependent influences on the morphology of individual neurons in more detail, we cultured dissociated hMNs on soft and rigid LN-PAA gels (Figure 2). We specifically focused on 0.5-kPa versus 25-kPa elasticities, as these are physiologically relevant elasticities comparable with CNS (0.5 kPa) and peripheral tissue (25 kPa) (Tyler, 2012). Consistent with observations of neurosphere cultures, isolated hMNs extended significantly longer neurites on rigid compared with soft substrata (Figures 2A–2D). However, hMNs generated significantly more primary neurites and branches on soft
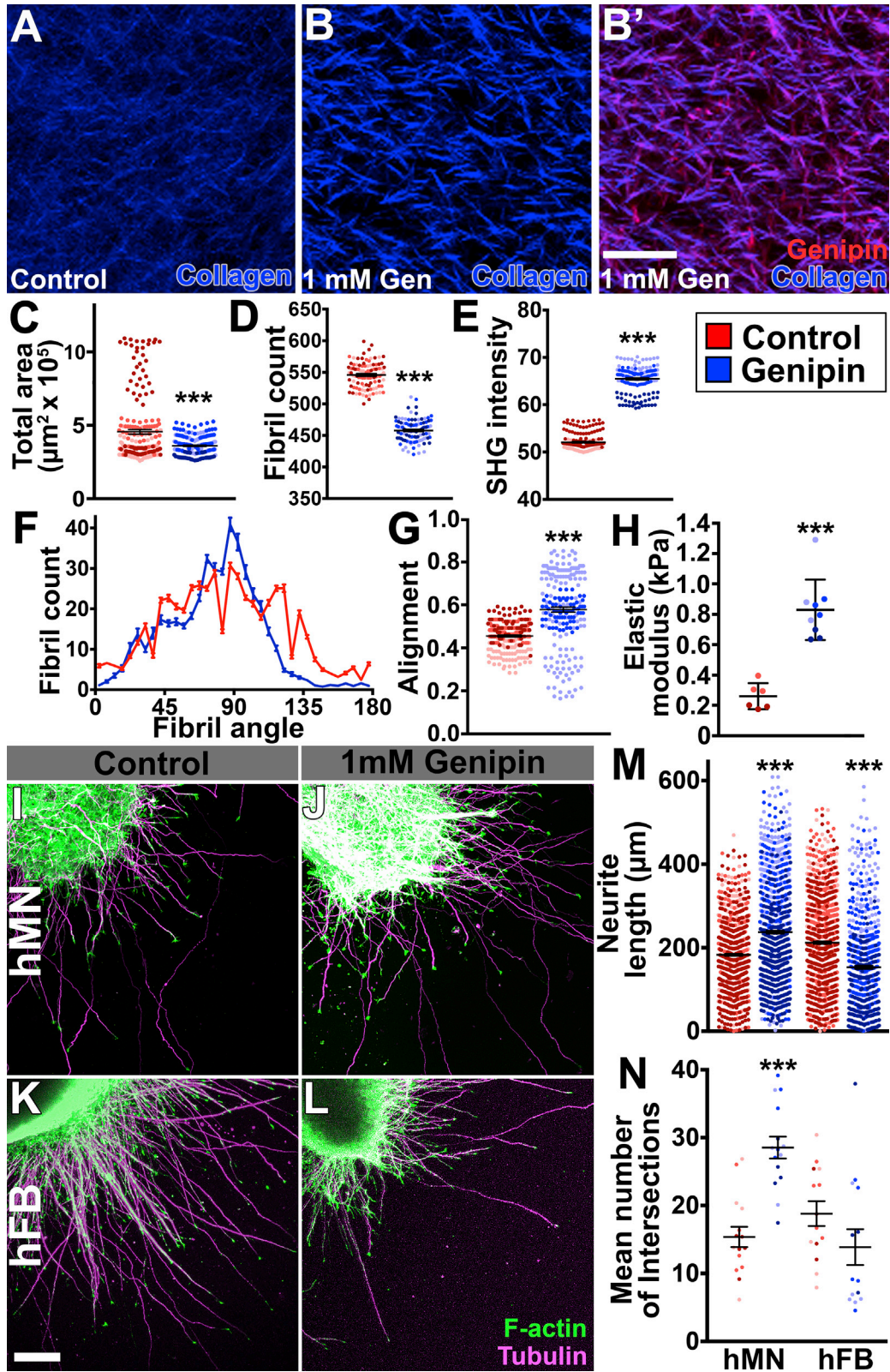
(legend on next page)

substrata (Figures 2E–2G). While these minor processes did not label for the dendrite-specific marker MAP2 (not shown), likely due to prematurity, these results are still consistent with enhanced dendritogenesis of MNs in soft, CNS-like elastic conditions and longer axons on rigid conditions, similar to the peripheral nervous system (PNS).

Neurite Extension by Human Neurons in 3D Collagen I Is Regulated by Substrata Elasticity

To further investigate the effect of environmental elasticity on neurite development, we examined neurite lengths in 3D collagen. Numerous studies have used collagen I matrices to study the effects of variable elastic conditions on cell shape, polarity, and durotaxis (Sundararaghavan et al., 2009; Willits and Skornia, 2004), as well as differentiation, neuritogenesis, and nerve regeneration (Gil and del Rio, 2012; Morelli et al., 2017; Musah et al., 2014). To test whether altering collagen elasticity affected hMN and hFB neurite outgrowth in three dimensions, we cultured neurospheres on top of 1.5 mg/mL fibrillar collagen I. This concentration of collagen produces dense matrices after 18 h of polymerization with peak linear modulus determined by tensile strength of the bulk material to be ~5 kPa (Roeder et al., 2002). On the other hand, using a nanoindentor (Optics11, Piuma, 9.5-μm radius probe), we determined the local elastic modulus of collagen polymerized under our conditions to be 260 ± 35 Pa (n = 6) after 18 h of polymerization. Note that local compression measurements are expected to be significantly lower than bulk tensile strength measurements (McKee et al., 2011). To investigate the effects of environmental rigidity on neurite outgrowth through 3D space, we polymerized collagen hydrogels together with 1 mM genipin for 18 h. Genipin is a natural collagen I crosslinking agent, which increases the rigidity of collagen I in a concentration-dependent and incubation-duration-dependent manner with little cytotoxic effects at low concentration (Sundararaghavan et al., 2008; Yunoki et al., 2013). Genipin was shown to increase the mechanical rigidity of collagen by 4- to 5-fold measured with parallel plate rheometry (Sundararaghavan et al., 2008), although we found only 3-fold increased rigidity measured by nanoindentation (829 ± 66 Pa, n = 9). Conveniently, genipin crosslinking of collagen is fluorogenic, providing a useful measure of crosslinking. Using two-photon microscopy, we viewed both genipin fluorescence (emission maximum 630 nm) and collagen structure, using collagen autofluorescence to visualize native collagen I fibrils by second harmonic generation (SHG) microscopy (Figures 3A–3B'). Using automated analysis software (CT-FIRE, see Experimental Procedures), we found that treating collagen I with genipin increased mean SHG fluorescence intensity, while reducing fibril number and area, but increased fiber alignment (Figures 3C–3G), compared with control-treated collagen I. Importantly, compression force measurements (Optics11) confirmed that collagen crosslinking by genipin increased collagen stiffness by 3-fold (Figure 3H).

Using genipin to crosslink collagen I, we examined the effects of varying matrix elasticity on hMN and hFB neurite outgrowth in three dimensions. Similar to our observations on LN-PAA, we found that hMNs extended longer neurites within more rigid, genipin-crosslinked collagen relative to control collagen after 4 days in culture (Figures 3I, 3J, and 3M). In contrast to hMNs, we found that hFB neurons extended significantly shorter processes within more rigid genipin-crosslinked collagen after 4 DIV relative to softer control conditions (Figures 3K–3M). Sholl analysis also showed significantly more hMN processes extending into rigid collagen (Figure 3N). Enhanced process extension of

Figure 3. Substratum Elasticity Influences Axon Development in Three-Dimensional Collagen I

(A–B') Maximum projections of multi-photon SHG volumetric images (35 slices covering 50 μm) of self-assembled 1.5 mg/mL collagen I hydrogels untreated (A) and crosslinked with 1 mM genipin (B). (B') SHG image of collagen (blue) merged with confocal genipin fluorescence image (excitation 620 nm, red). Note strong colocalization of the collagen fibrils with genipin and reduced fibril density compared with control.

(C–E) The total area occupied by collagen fibrils (C) and fibril count (D) are significantly reduced in genipin-treated hydrogels compared with untreated, while mean SHG intensity (E) is increased.

(F and G) Fibril orientation becomes less variable (F) and total fibril alignment (G) is increased by genipin treatment. All collagen fibril measurements were made using CT-FIRE software on three hydrogels per condition (see Experimental Procedures).

(H) Elastic modulus measured using a nanoindentation device (see Experimental Procedures). n = 2–3 hydrogels for each condition.

(I–L) Low-magnification confocal z-stack images of hMN (I and J) and hFB (K and L) neurospheres immunolabeled for acetylated tubulin (magenta) and F-actin (phalloidin, green). Neurospheres were cultured on untreated (I and K) and genipin-crosslinked collagen hydrogels (J and L) for 4 DIV.

(M) Quantification of neurite lengths on control collagen and collagen with genipin for hMN and hFB. Note the opposite effect on neurite length for hMN and hFB on soft and stiff collagen. n ≥ 755 neurites from n = 3 experiments from n = 2 differentiations for each condition.

(N) Sholl analysis of mean number of intersections shows that there are more intersecting neurites on more rigid substrata for hMNs. n ≥ 700 neurites from n = 3 experiments from n = 3 differentiations for each condition.

***p < 0.001, Student's t test. Scale bars, 40 μm (A and B) and 100 μm (I–L).
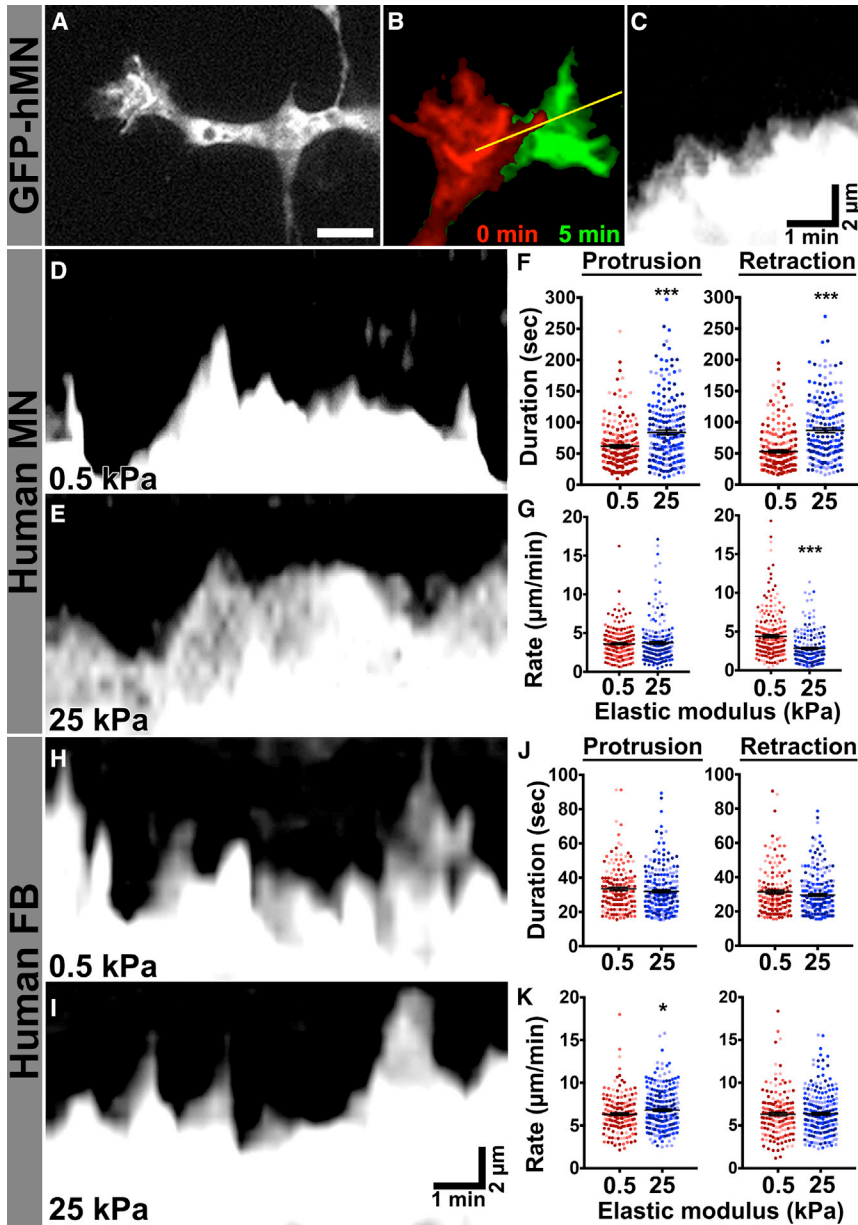
Figure 4. The Stability of Lamellipodial Protrusions by hMN and hFB Growth Cones Depends on Substratum Rigidity

(A) A GFP-expressing hMN growth cone on rigid LN-PAA.

(B) Two-time-point image merge of growth cone in (A) at times indicated showing initial (red) and final (green) position. Yellow line indicates line used to produce kymograph from 5-min time-lapse sequence.

(C) Kymograph constructed from region specified in (B) showing protrusion and retraction events.

(D and E) Representative kymographs generated from hMN growth cone lamellipodial protrusions on soft (D) and rigid substrata (E). Note greater stability of leading-edge protrusions on rigid substratum.

(F) Duration of protrusion and retraction events on soft and rigid substrata for hMN growth cones.

(G) Rate of membrane protrusion and retraction of hMN growth cone leading edge on soft and rigid substrata.

(H and I) Representative kymographs generated from hFB growth cone lamellipodial protrusions on soft (H) and rigid (I) substrata. Note unstable leading-edge protrusions on soft and rigid substrata.

(J) Duration of protrusion and retraction events on soft and rigid substrata for hFB growth cones.

(K) Rate of membrane protrusion and retraction of hFB growth cone leading edge on soft and rigid substrata. Note that protrusion durations and rates are significantly different between hMNs and hFB neurons.

n $\geq$ 164 kymographs from n = 3 experiments from n = 2 differentiations for each condition. ***p < 0.001, *p < 0.01, Student's t test. Scale bars, 10 μm (A) and 5 um (B).

hFB neurons within soft 3D collagen may be related to the affinity of collagen as a ligand (relative to 2D LN) or may be due to specific sensitivities of hFB growth cones to 3D mechanical environments, which were over a softer mechanical range than observations made in two dimensions. While the precise nature of interactions of growth cones with collagen I fibrils in three dimensions is unclear, it is important to note that since collagen pore size appears larger than axons in both conditions (Figures 3A–3B′), this factor is unlikely to contribute to differential effects on neurite outgrowth. Taken together, our results suggest that 3D environmental elasticity regulates human neuritogenesis in a neuronal subtype-dependent manner.

Rigid Substrata Stabilize Growth Cone Leading-Edge Protrusions

To begin to address whether differences in growth cone leading-edge adhesion may be responsible for rigidity-dependent neurite outgrowth, we compared protrusion dynamics of GFP-expressing hMNs and hFB neurons by kymography. Fluorescent hMNs and hFB neurons on soft (0.5 kPa) and rigid (25 kPa) LN-PAA gels were imaged at 1 DIV every 5 s for 5 min by fluorescence microscopy. Protrusions were quantified by sampling 3–5 five kymographic lines per growth cone (Figures 4A–4C). Kymographic analysis showed that hMN growth cones had longer-lived protrusions on rigid substrata compared with soft (Figures 4D and 4E), indicated by

prolonged protrusion duration and retraction, as well as slower rates of leading-edge retraction (Figures 4F and 4G). However, we found that the protrusion rates by hMNs on soft and rigid substrata did not differ (Figure 4G), suggesting that the rate of actin polymerization may not be affected by substrata elasticity. In contrast to hMNs, we found that hFB neurons showed no elasticity-dependent effects on protrusion lifetime (Figures 4H–4J), suggesting that substratum elasticity does not influence adhesion in CNS projecting neurons, which may be due to a lack of integrin-mediated adhesions made by CNS neurons compared with PNS neurons (Koch et al., 2012). While hFB growth cones did show slightly faster protrusion rates on rigid substrata (Figure 4K), this does not explain more rapid neurite outgrowth on soft relative to rigid substrata (Figure 1S). It is important to note that the durations of protrusion and retraction were significantly shorter by hFB neurons compared with hMNs, suggesting an overall reduction of adhesive influence on hFB outgrowth (Figures 4F and 4J). Together, these data suggest that CNS growth cone motility may be more dependent on direct regulation of the cytoskeleton, whereas peripheral projecting neurite development is more strongly influenced by growth cone substratum adhesion.

### RHOA and Myosin II Activity Are Elevated in hMNs on Rigid Substrata

To begin to address mechanisms of rigidity-dependent axon extension, we focused the remainder of this study on comparing hMNs on soft and rigid substrata, as these neurons showed the most robust differences in 2D conditions. Rho family GTPases can both positively and negatively influence neurite extension downstream of chemical cues (Gomez and Letourneau, 2014; Hall and Lalli, 2010), and RHOA activity is also regulated by the mechanical environment for many cell types (Lessey et al., 2012), including developing neurons (Chang et al., 2017). For example, RHOA activation of Rho-associated protein kinase (ROCK) and myosin II contractility supports the maturation of cell-substratum adhesions (Schiller and Fassler, 2013; Woo and Gomez, 2006), which sense the elastic cell substratum through mechanically gated ion channels and integrin receptors (Kerstein et al., 2013; Vicente-Manzanares et al., 2009). Moreover, contractile forces transmitted to integrin receptors provide homeostatic feedback that affects RHOA activity through specific guanine nucleotide exchange factors (Lawson and Burridge, 2014; Lessey et al., 2012). To address whether similar feedback mechanisms may operate in developing human neurons, we compared RHOA activity in hMNs cultured on soft (0.5 kPa) and rigid (25 kPa) substrata, as well as ROCK activity by measuring phosphorylation of its primary target, myosin light chain (MLC), at activation site Ser19. Comparing protein extracts from hMNs cultured on soft and rigid LN substrata, we found that

RHOA is more active in neurons cultured on rigid substrata (Figure 5A). Since measuring active RHOA in whole-cell extracts does not reveal local activity within growth cones, we used immunocytochemistry (ICC) to measure pS19-MLC, a downstream target of RHOA/ROCK signaling. Consistent with elevated active RHOA, we found that pS19-MLC is higher in hMN axons and growth cones on rigid compared with soft substrata (Figures 5B–5F). Importantly, we validated S19-MLC as an accurate readout of RHOA activity by showing that pharmacological activation of RHOA with lysophosphatidic acid (LPA) and inhibition with Rho Inhibitor I (C3 transferase) modulated S19-MLC accordingly (Figures 5G and 5H). It is important to note that growth cone size does not account for differences observed in RHOA signaling, as the average growth cone area on soft (140.5 ± 7 μm^2) is similar to rigid (145.7 ± 9 μm^2) substrata.

Activation of Adhesion Proteins Correlates with Rigidity-Dependent Neurite Outgrowth

As adhesion/stabilization of protrusions appears to support hMN neurite outgrowth on rigid substrata (Figure 4), we examined whether elasticity-dependent intracellular signals correlate with adhesion of hMN growth cones. Upon integrin activation and clustering, the non-receptor tyrosine kinases SRC and FAK phosphorylate nascent adhesion proteins talin, paxillin, and p130-CAS (Sawada et al., 2006), which may depend on mechanical forces (Moore et al., 2010). The dynamic assembly and turnover of adhesions depends on tyrosine phosphorylation of these adhesion proteins, which promote cell motility and neurite extension (Kerstein et al., 2015). To test how adhesion signaling within hMN growth cones may regulate elasticity-dependent neurite outgrowth, we measured adhesion protein phosphorylation of hMNs on soft and rigid PAA substrata. We found that both FAK (pY397) and SRC (pY418) are more active within hMN growth cones on rigid substrata relative to soft substrata (Figures 6A–6D, 6K, 6L, S5A, and S5B). Conversely, tyrosine phosphorylation of the inhibitory site of SRC (pY529) was higher on soft relative to rigid substrata (Figures 6E, 6F, 6M, and S5C). Active SRC, in association with FAK, phosphorylates the adaptor protein p130-CAS that requires mechanical strain to expose cryptic tyrosine residues (Moore et al., 2010; Sawada et al., 2006). We immunolabeled two cryptic activation sites of p130-CAS, namely pY165 and pY410, to assess changes in p130-CAS activity. Consistent with activation of FAK and SRC, we observed significantly higher phosphorylation at Y165 and at Y410 of p130-CAS in hMN growth cones on rigid substrata compared with soft (Figures 6G–6J, 6N, 6O, S5D, and S5E). These observations show that elasticity-dependent activation of adhesion signaling and
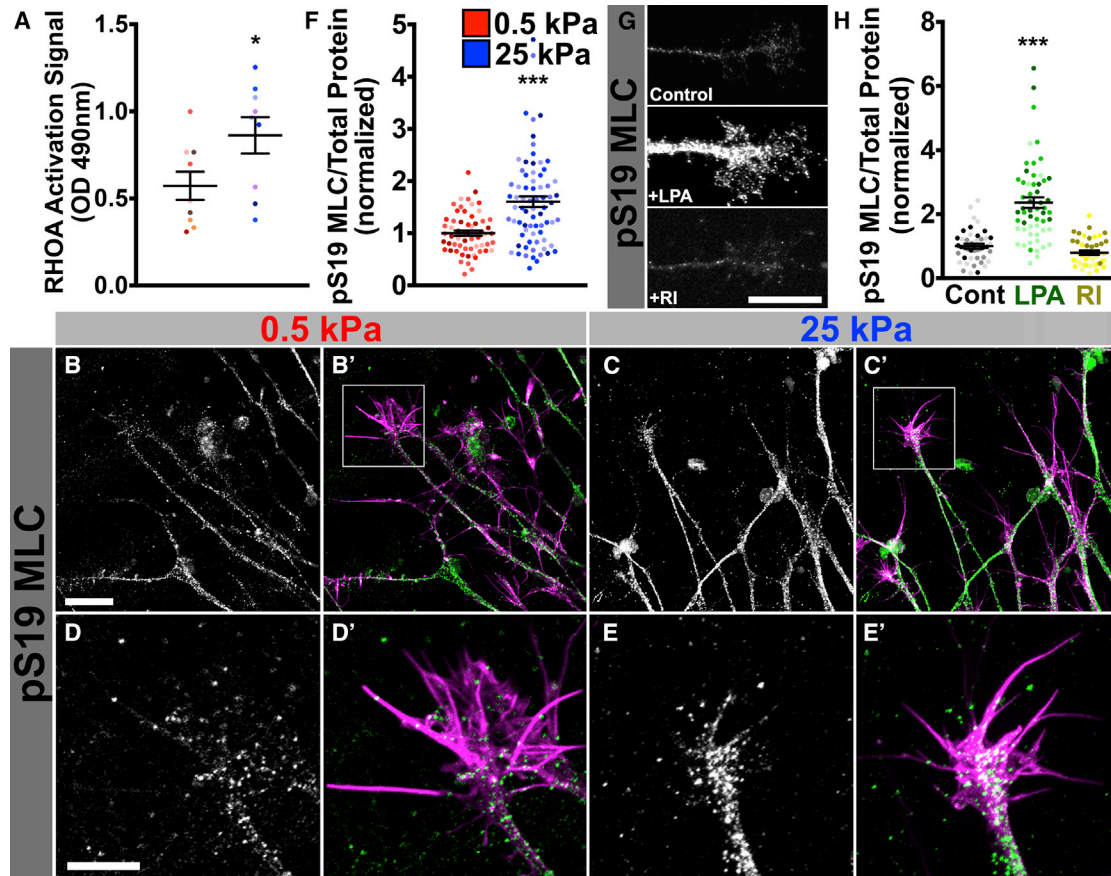
Figure 5. RHOA and MLC Activities Are Increased in hMNs on Rigid Substrata

(A) Biochemical measurement of active RHOA in hMNs cultured on soft and rigid PAA hydrogels shows RHOA activity is higher in hMNs on rigid substrata. n = 9 replicates from n = 5 experiments for each condition. *p < 0.01, Student's t test.

(B–C') Representative confocal fluorescent images of hMN neurites on soft (B and B') and rigid (C and C') LN-coated PAA hydrogels. Neurons were immunolabeled with phospho-specific MLC antibodies at the activation site Ser19 (green in merge) and co-labeled for F-actin (phalloidin, magenta). Note increased pS19-MLC labeling in axons and growth cones on rigid PAA hydrogels.

(D–E') Zoomed images (from boxes indicated in B' and C') showing hMN growth cones on soft (D and D') and rigid (E and E') substrata.

(F) Quantification of pS19-MLC fluorescence intensities in hMN growth cones on soft and rigid PAA hydrogels. Measurements of pS19-MLC fluorescence are normalized to total protein labeling (see Experimental Procedures). n ≥ 50 growth cones from n = 3 experiments from n ≥ 2 differentiations for each condition. ***p < 0.001, Student's t test.

(G) Confocal images of growth cones of hMNs cultured on LN-coated glass and stimulated for 1 h with control medium (top), 100 nM LPA (middle), or 2 μg/mL Rho Inhibitor I (bottom), then immunolabeled for pS19-MLC. Note robust pS19-MLC labeling of growth cone treated with LPA.

(H) pS19-MLC fluorescence intensity measurements of hMN growth cones. n ≥ 43 growth cones from n = 3 experiments from n ≥ 2 differentiations for each condition. ***p < 0.001, Student's t test.

Scale bars, 20 μm (B and C) and 10 μm (D, E, and G).

scaffolding proteins correlates with increased hMN neurite outgrowth on rigid substrata.

Modulating RHOA Activity in hMNs Regulates Mechanosensitive Neurite Outgrowth

To assess the importance of RHOA activity during elasticity-dependent growth cone motility in hMNs, we tested the effects of acute pharmacological manipulation of RHOA activity on neurite length, rate of outgrowth, and membrane protrusion on soft and rigid substrata. LPA is a signaling lipid that binds G-protein-coupled receptors to activate RHOA, which induces robust growth cone collapse at high doses on rigid substrata (Fincher et al., 2014), but the effects of LPA on neurite extension on flexible substrata has not been examined. We first tested the effects of chronic RHOA activation using LPA on hMNs on soft and
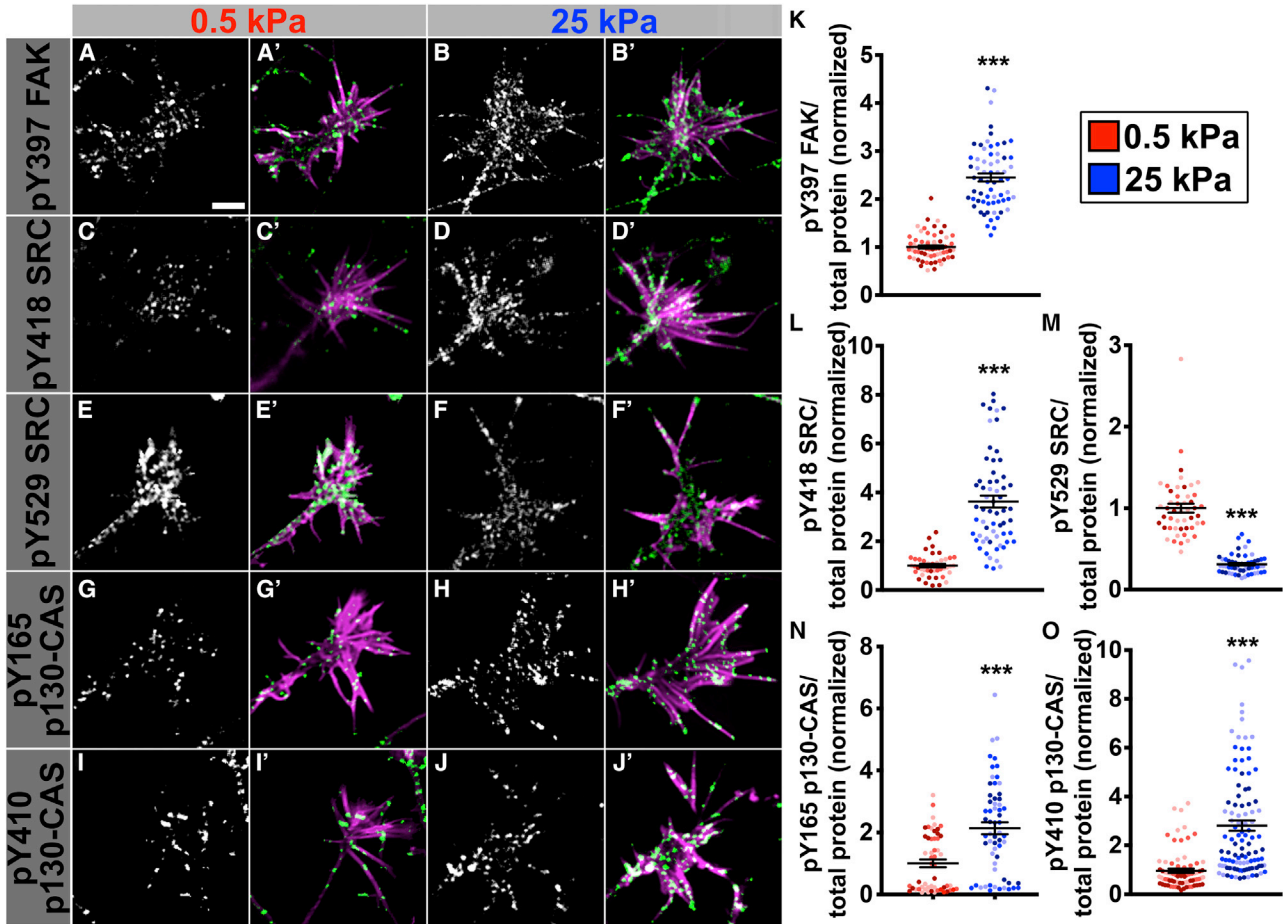
Figure 6. Activation of Adhesion Signaling and Scaffolding in hMN Growth Cones on Rigid Substrata

(A–J') Representative confocal images of hMN growth cones on soft (A, C, E, G, and I) and rigid (B, D, F, H, and J) LN-coated PAA gels. Neurons were immunolabeled with phospho-specific antibodies (green in merges) to the sites indicated and counterstained for F-actin (phalloidin, magenta). Scale bar, 5 μm.

(K–O) Fluorescence intensity measurements for activation sites for FAK (y397) (K), SRC (y418) (L), and p130-CAS (y165 [N] and y410 [O]), and an inhibitory site of SRC (y529) (M). Measurements of phosphorylated adhesion proteins are presented as ratio against total protein labeling using SE647 (see Experimental Procedures) in hMN growth cones at specified phosphorylation sites, and ratio measurements of neurons on rigid substrata data are normalized to soft substrata. n ≥ 44 growth cones for each labeling from n = 3 experiments from n ≥ 2 differentiations for each condition. ***p < 0.001, Student's t test.

See also Figure S5.

rigid substrata over 24 h. Surprisingly, we found that LPA caused a significant and dose-dependent increase in neurite lengths of hMNs on soft substrata (Figures 7A, 7B, 7G, S6A–S6D, and S6I), but reduced neurite lengths by the same neurons on more rigid substrata (Figures 7D, 7E, 7G, and S6E–S6I). Considering our findings that RHOA is less active in neurons on soft compared with rigid substrata (Figure 5), these results suggest that the mechanical environment sets the baseline RHOA activity, which can be further optimized to promote maximal neurite extension rates. If true, we hypothesized that RHOA inhibition would have the opposite effects on neurite extension by hMNs

on rigid and soft substrata compared with RHOA activation. Using Rho Inhibitor I, which inhibits RHOA, RHOB, and RHOC (Sahai and Olson, 2006), we found that chronic RHOA inhibition of developing hMNs increased neurite lengths after 24 h on rigid substrata, while neurite lengths are significantly reduced on soft substrata with the same treatment (Figures 7C, 7F, and 7G). While the RHOA modulators we used may have additional targets, the opposing effects of two different pharmacological modulators on outgrowth suggest that RHOA is the likely target and are consistent with the importance of balanced RHOA activity for optimal, substratum-dependent neurite extension.
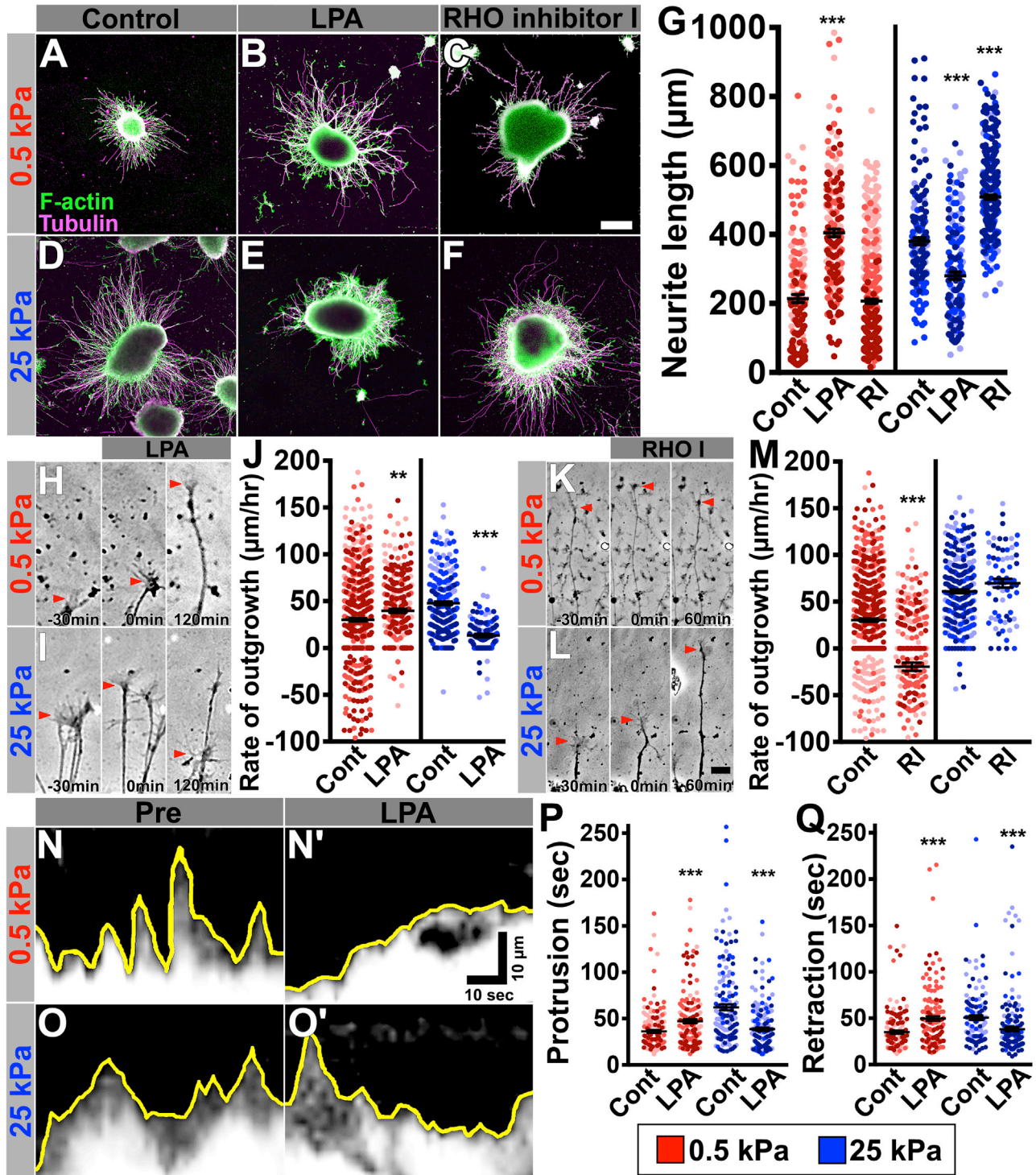
Figure 7. Modulating RHOA Signals Switches the Effects of Elastic Substrata on hMN Neurite Outgrowth

(A–F) Representative images of hMN neurospheres after 2 DIV on soft (A–C) and rigid (D–F) substrata. hMNs were treated with control medium (A and D), 100 nM LPA (B and E), or 2 μg/mL Rho Inhibitor I (C and F) for 24 h, then fixed and immunolabeled for acetylated tubulin (magenta) and F-actin (phalloidin, green).

(G) Mean neurite lengths of hMNs upon chronic modulation of RHOA reveals opposing effects that depend on substrata elasticity. $n \geq 100$ longest neurites from $n = 3$ experiments from $n = 3$ differentiations for each condition. ***$p < 0.001$, one-way ANOVA.

(legend continued on next page)

To distinguish between the possible effects of altered long-term RHOA signaling on neuronal differentiation (Musah et al., 2014; Stankiewicz and Linseman, 2014), we used live-cell imaging to measure neurite extension rates during acute modulation of RHOA activity. Under normal conditions, hMN neurite outgrowth is faster on rigid than on soft substrata (Figures 1N–1P). However, upon acute treatment with 100 nM LPA, hMN neurite extension accelerated on soft, but decelerated on rigid substrata (Figures 7H–7J). It is important to note that we observed transient retraction of all neurites in response to LPA on both soft and rigid substrata, but neurites on soft substrata quickly recovered to extend more rapidly, while neurites on rigid substrata slowly recovered and extended more slowly. In contrast to RHOA activation, acute Rho inhibition with 2 μg/mL Rho Inhibitor I had opposite effects on neurite extension, as neurite outgrowth was further reduced on soft substrata (Figures 7K and 7M) but modestly increased on rigid substrata (Figures 7L and 7M). These results suggest that the mechanical environment modulates local RHOA activity in growth cones to control force-dependent neurite outgrowth.

Balanced RHOA activity is necessary for maximal neurite outgrowth, as RHOA both inhibits growth cone motility by increasing F-actin retrograde flow (Nichol et al., 2016) and supports motility by promoting substratum adhesion (Woo and Gomez, 2006). To assess the role of RHOA on elasticity-dependent growth cone adhesion, we examined the stability of leading-edge protrusions during acute activation of RHOA on soft and rigid substrata. Kymographs were generated from time-lapse fluorescence movies of GFP-expressing hMN growth cones before and 30 min post LPA treatment (during recovery phase). On soft substrata, leading-edge protrusions were unstable with rapid protrusion and retraction events (Figure 7N), which stabilized after LPA treatment (Figures 7N′, 7P, and 7Q). In contrast, on rigid substrata, LPA treatment destabilized leading-edge protru-

sions, possibly due to increased retrograde flow or de-adhesion (Figures 7O–7Q). Taken together, these data indicate that RHOA provides homeostatic feedback in response to environment elasticity in human nerve growth cones and may control axon pathfinding based on local differences in tissue elasticity.

RHOA Signaling Mediates Elasticity-Dependent Phosphorylation of Mechanosensitive Adhesion Proteins

Acute activation of RHOA accelerates hMN neurite outgrowth on soft but reduces outgrowth on rigid substrata (Figures 7H–7J), suggesting that RHOA influences elasticity-dependent adhesion signaling. To test this, we acutely activated RHOA in hMNs on soft and rigid substrata and measured phosphorylation of FAK, SRC, and p130-CAS by quantitative ICC. Unexpectedly, acute treatment of hMNs with 100 nM LPA for 1 h significantly decreased pY-397 FAK in growth cones on both soft (Figures S7A, S7C, and S7M) and rigid substrata (Figures S7B, S7D, and S7M). However, RHOA activation increased pY-418 SRC on soft substrata (Figures S7E, S7G, and S7N) but decreased pY-418 SRC on rigid substrata (Figures S7F, S7H, and S7N). Similar to FAK, we found that RHOA activation with LPA reduced p130-CAS phosphorylation at pY165 in growth cones on soft substrata (Figures S7I, S7K, and S7O) and rigid substrata (Figures S7J, S7L, and S7O). Taken together, these data show that RHOA has complex upstream effects on FAK, SRC, and p130-CAS that depend on the mechanical environment.

DISCUSSION

Here, we compared peripheral projecting hMNs and CNS-resident hFB neurons differentiated from iPSCs and found that these distinct classes of human neurons

---

(H and I) Time-lapse differential interference contrast (DIC) images of live hMNs of soft (H) and rigid (I) substrata at time points indicated before and after treatment with 100 nM LPA.

(J) Rate measurements show that LPA treatment significantly increases outgrowth on soft substrata, but reduces outgrowth on rigid substrata. n ≥ 116 neurites from n = 3 experiments from n = 2 differentiations for each condition. ***p < 0.001, **p < 0.05, Student's t test.

(K and L) Time-lapse DIC images of live hMNs of soft (K) and rigid (L) substrata at time points indicated before and after treatment with 2 μg/mL Rho Inhibitor I.

(M) Rate measurements show that RHOA inhibition significantly reduces outgrowth on soft substrata, but modestly increases outgrowth on rigid substrata. n ≥ 69 neurites from n = 3 experiments from n = 2 differentiations for each condition. ***p < 0.001, Student's t test.

(N–O′) Kymographs generated from GFP-expressing hMN growth cones on soft and rigid substrata before and after acute activation of RHOA with 100 nM LPA. Note increased stability of the leading edge (yellow line) on soft substrata after LPA treatment (N′).

(P and Q) Leading-edge membrane protrusion duration (P) and retraction (Q) events on soft and rigid substrata for hMN growth cones before and after 100 nM LPA. Note significant increase in duration of protrusion and retraction after LPA on soft substrata but decrease on rigid substrata. n ≥ 141 kymographs from n = 3 experiments from n = 2 differentiations for each condition. ***p < 0.001, Student's t test. Scale bars, 100 μm (A–F) and 10 μm (H, I, K, and L). See also Figure S6.

exhibited specific sensitivities to the mechanical properties of their extracellular environment. Using 2D PAA (Figures 1 and 2) and 3D collagen hydrogels (Figure 3) of varying elasticity, we found that developing hMNs extended longer processes and showed faster neurite outgrowth on rigid substrata. Importantly, hMNs extended neurites maximally at 25 kPa PAA, which is comparable with the elasticity of muscle tissue (Tyler, 2012). In contrast, while substrata elasticity did not significantly influence hFB neurite outgrowth on 2D environments, hFB neurons extended longer neurites in soft 3D collagen I matrices. Strong adhesion of leading-edge protrusions (Figure 4) appear responsible for fast neurite extension by hMNs on rigid substrata, which correlated with increased activation of RHOA, MLC, FAK, SRC, and p130-CAS (Figures 5 and 6). Consistent with our evidence that substratum elasticity regulates basal RHOA activity in growth cones, we found that elevating RHOA activity can alter mechanosensitive responses within elastic environments, as LPA caused hMNs to extend longer neurites on soft substrata but reduced process extension on rigid substrata (Figure 7). Changes in RHOA activity resulted in downstream modulation of FAK, SRC, and p130 Cas function, which may be responsible for substratum elasticity-dependent effects on neurite outgrowth. Together, our results show for the first time that the mechanical properties of the environment control the growth of developing human neurons through homeostatic regulation of RHOA.

There are still many open questions regarding the mechanisms and roles of tissue elasticity in neuronal differentiation and network assembly. Our current data, together with previous findings (Balgude et al., 2001; Cheng et al., 2011; Flanagan et al., 2002; Jiang et al., 2008; Kerstein et al., 2013; Koch et al., 2012; Kostic et al., 2007; Sundararaghavan et al., 2009; Willits and Skornia, 2004), suggest that the biophysical properties of the environment may be a critical regulator of axon development (Barriga et al., 2018). Tissue rigidity varies greatly throughout embryos, providing a complex and dynamic mechanical environment for developing axons and dendrites (Elkin et al., 2007; Koser et al., 2016). Neuronal differentiation and axon extension must occur over a wide range of tissue elasticities, from extremely soft, such as brain (Young's modulus = 100–1,000 Pa), to more rigid, such as vascular tissue and bone (30 kPa and 20 GPa, respectively), covering and impressive >1 × 10^6-fold range of elasticities (Kohn et al., 2015; Kruse et al., 2008; Tyler, 2012). Moreover, mounting evidence suggests that there are regional differences in brain tissue elasticity due to composition and organization of the ECM, as well as cell-type heterogeneity. For example, region-dependent variations in tissue rigidity were discovered in *Xenopus* optic tectum using atomic force microscopy (Koser et al., 2016). Interestingly, developing retinal ganglion cell (RGC) axons appear to be guided by this elasticity gradient, as they grow into softer tectal regions and guidance errors occur if graded tissue elasticity is disrupted. It is also noteworthy that FAK signaling is involved in retinotopic mapping of RGC axons (Woo et al., 2009).

While the precise mechanisms of cellular mechanosensing remain poorly understood, integrin-based adhesion is critical to force sensing and transmission of force-dependent signals into most cells (Geiger et al., 2009; LaCroix et al., 2015; Sun et al., 2016; Oria et al., 2017). Similar to non-neuronal cells, our data indicate that RHOA, myosin II, FAK, SRC, and p130-Cas signals are critical regulators downstream of cell adhesion in growth cones. Integrin activation and clustering lead to recruitment of multiple signaling and scaffold molecules, such as SRC and FAK, which subsequently phosphorylate adhesion proteins, including paxillin and p130-Cas (Chang et al., 2017; Cohen-Hillel et al., 2009; Myers and Gomez, 2011; Robles and Gomez, 2006; Sawada et al., 2006). Full maturation of adhesions results in coupling with the actin cytoskeleton and clutching of F-actin retrograde flow (RF) to produce cellular traction forces (Chan and Odde, 2008; Lin et al., 1996; Lin and Forscher, 1995; Nichol et al., 2016). Traction force provided by myosin II-dependent RF coupling to adhesions further activates proteins such as SRC and FAK (Bae et al., 2014; Wang et al., 2005), which are influenced substratum rigidity (Paszek et al., 2005; Shimizu et al., 2014). Downstream target proteins, such as p130-Cas, are mechanically stretched by actin RF, revealing cryptic SRC phosphorylation sites (Kostic et al., 2007; Moore et al., 2010; Sawada et al., 2006). Finally, upstream regulation of myosin II contractility by RHOA/ROCK signaling is also influenced by substratum rigidity, creating a homeostatic feedback between RHOA-mediated contraction, adhesion stabilization, and traction force (Kshitiz et al., 2012; Paszek et al., 2005) (Figure S9). Importantly, recent molecular modeling studies predict that the elasticity optimum for cell migration can be shifted by modulating motors and clutches (adhesion proteins) (Bangasser et al., 2013, 2017). Our results suggest that human neurite development is also influenced by homeostatic feedback through adhesive interactions with their elastic environment. Moreover, we predict that hFB neurons and hMNs have specific complements of adhesion receptors, clutch proteins, and motors that allow optimal outgrowth on soft and more rigid substrata, respectively. Future work should aim to identify the specific adhesion proteins, clutches, molecular motors, and upstream modulators that may be responsible for different sensitivities of hMNs and hFB neurons to their elastic environment.

EXPERIMENTAL PROCEDURES

Neuronal Differentiation, Dissociation, and Transfection

hFB neurons and hMNs were differentiated as previously described (Doers et al., 2014; Du et al., 2015; Hu et al., 2010). Neurospheres were plated onto 2D polyacrylamide (PAA) hydrogels (Matrigen) coated first with 50 μg/mL PDL followed by either 25 μg/mL LN (Sigma-Aldrich) or 10 μg/mL fibronectin (Sigma-Aldrich). These functionalized gels bind ECM proteins equivalently across elasticities (Matrigen communication), which we confirmed with LN binding (Figure S1). Collagen I (Corning) was polymerized at 1.5 mg/mL according to the manufacturer's recommendation and was crosslinked using 1 mM genipin (Sigma-Aldrich) for 18 h followed by extensive rinsing in culture medium. Neurons were imaged or fixed at 1 DIV or 4 DIV for 2D and 3D cultures, respectively.

Immunocytochemistry

Neuronal cultures were fixed in 4% paraformaldehyde in Krebs sucrose fixative (Dent and Meiri, 1992), permeabilized with 0.1% Triton X-100, and blocked in 1.0% fish gelatin in calcium-magnesium-free PBS for 1 h at room temperature.

RHOA G-LISA

An RHOA G-LISA activation assay colorimetric kit (Cytoskeleton) was used to measure RHOA activity in hMNs.

Image Analysis

Images were analyzed using ImageJ software (W. Rasband, National Institutes of Health, Bethesda, MD). To measure protrusion dynamics, we imaged GFP-expressing hMN growth cones at 2 Hz by wide-field fluorescence microscopy for 2 min. Leading-edge morphology was quantified by kymography. Automated measurements of collagen fibril orientation, alignment, and fibril number were performed using CT-FIRE software developed at the Laboratory for Optical and Computational Instrumentation at the University of Wisconsin-Madison (Bredfeldt et al., 2014).

Sholl Analysis

Images were analyzed using the Sholl Analysis (Sholl and Uttley, 1953) plugin in ImageJ.

Statistical Analysis

Analysis was carried out using Prism software. Analysis was completed using unpaired Student's t tests for comparison of two experimental groups, or a one-way or two-way ANOVA with a Bonferroni's multiple-comparison test for comparison of three or more experimental groups.

SUPPLEMENTAL INFORMATION

Supplemental Information can be found online at https://doi.org/10.1016/j.stemcr.2019.10.008.

REFERENCES

Bae, Y.H., Mui, K.L., Hsu, B.Y., Liu, S.L., Cretu, A., Razinia, Z., Xu, T., Puré, E., and Assoian, R.K. (2014). A FAK-Cas-Rac-lamellipodin signaling module transduces extracellular matrix stiffness into mechanosensitive cell cycling. Sci Signal 7, ra57.

Balgude, A.P., Yu, X., Szymanski, A., and Bellamkonda, R.V. (2001). Agarose gel stiffness determines rate of DRG neurite extension in 3D cultures. Biomaterials 22, 1077–1084.

Bangasser, B.L., Rosenfeld, S.S., and Odde, D.J. (2013). Determinants of maximal force transmission in a motor-clutch model of cell traction in a compliant microenvironment. Biophys. J. 105, 581–592.

Bangasser, B.L., Shamsan, G.A., Chan, C.E., Opoku, K.N., Tuzel, E., Schlichtmann, B.W., Kasim, J.A., Fuller, B.J., McCullough, B.R., Rosenfeld, S.S., et al. (2017). Shifting the optimal stiffness for cell migration. Nat. Commun. 8, 15313.

Barriga, E.H., Franze, K., Charras, G., and Mayor, R. (2018). Tissue stiffening coordinates morphogenesis by triggering collective cell migration in vivo. Nature 554, 523–527.

Bonanomi, D., and Pfaff, S.L. (2010). Motor axon pathfinding. Cold Spring Harb. Perspect. Biol. 2, a001735.

Bredfeldt, J.S., Liu, Y., Conklin, M.W., Keely, P.J., Mackie, T.R., and Eliceiri, K.W. (2014). Automated quantification of aligned collagen for human breast carcinoma prognosis. J. Pathol. Inform. 5, 28.

Chan, C.E., and Odde, D.J. (2008). Traction dynamics of filopodia on compliant substrates. Science 322, 1687–1691.

Chang, T.Y., Chen, C., Lee, M., Chang, Y.C., Lu, C.H., Lu, S.T., Wang, D.Y., Wang, A., Guo, C.L., and Cheng, P.L. (2017). Paxillin facilitates timely neurite initiation on soft-substrate environments by interacting with the endocytic machinery. Elife 6.

Cheng, C.M., LeDuc, P.R., and Lin, Y.W. (2011). Localized bimodal response of neurite extensions and structural proteins in dorsal-root ganglion neurons with controlled polydimethylsiloxane substrate stiffness. J. Biomech. *44*, 856–862.

Cohen-Hillel, E., Mintz, R., Meshel, T., Garty, B.Z., and Ben-Baruch, A. (2009). Cell migration to the chemokine CXCL8: Paxillin is activated and regulates adhesion and cell motility. Cell. Mol. Life Sci. *66*, 884–899.

De Wit, J., De Winter, F., Klooster, J., and Verhaagen, J. (2005). Semaphorin 3A displays a punctate distribution on the surface of neuronal cells and interacts with proteoglycans in the extracellular matrix. Mol. Cell. Neurosci. *29*, 40–55.

Dent, E.W., and Meiri, K.F. (1992). GAP-43 phosphorylation is dynamically regulated in individual growth cones. J. Neurobiol. *23*, 1037–1053.

Doers, M.E., Musser, M.T., Nichol, R.H., Berndt, E.R., Baker, M., Gomez, T.M., Zhang, S.C., Abbeduto, L., and Bhattacharyya, A. (2014). iPSC-derived forebrain neurons from FXS individuals show defects in initial neurite outgrowth. Stem Cells Dev. *23*, 1777–1787.

Du, Z.W., Chen, H., Liu, H., Lu, J., Qian, K., Huang, C.L., Zhong, X., Fan, F., and Zhang, S.C. (2015). Generation and expansion of highly pure motor neuron progenitors from human pluripotent stem cells. Nat. Commun. *6*, 6626.

Elkin, B.S., Azeloglu, E.U., Costa, K.D., and Morrison, B., 3rd. (2007). Mechanical heterogeneity of the rat hippocampus measured by atomic force microscope indentation. J. Neurotrauma *24*, 812–822.

Fincher, J., Whiteneck, C., and Birgbauer, E. (2014). G-protein-coupled receptor cell signaling pathways mediating embryonic chick retinal growth cone collapse induced by lysophosphatidic acid and sphingosine-1-phosphate. Dev. Neurosci. *36*, 443–453.

Flanagan, L.A., Ju, Y.E., Marg, B., Osterfield, M., and Janmey, P.A. (2002). Neurite branching on deformable substrates. Neuroreport *13*, 2411–2415.

Franze, K. (2013). The mechanical control of nervous system development. Development *140*, 3069–3077.

Geiger, B., Spatz, J.P., and Bershadsky, A.D. (2009). Environmental sensing through focal adhesions. Nat. Rev. Mol. Cell Biol. *10*, 21–33.

Gil, V., and del Rio, J.A. (2012). Analysis of axonal growth and cell migration in 3D hydrogel cultures of embryonic mouse CNS tissue. Nat. Protoc. *7*, 268–280.

Gomez, T.M., and Letourneau, P.C. (2014). Actin dynamics in growth cone motility and navigation. J. Neurochem. *129*, 221–234.

Gomez, T.M., Roche, F.K., and Letourneau, P.C. (1996). Chick sensory neuronal growth cones distinguish fibronectin from laminin by making substratum contacts that resemble focal contacts. J. Neurobiol. *29*, 18–34.

Hall, A., and Lalli, G. (2010). Rho and Ras GTPases in axon growth, guidance, and branching. Cold Spring Harb Perspect. Biol. *2*, a001818.

Hu, H. (2001). Cell-surface heparan sulfate is involved in the repulsive guidance activities of Slit2 protein. Nat. Neurosci. *4*, 695–701.

Hu, B.Y., Weick, J.P., Yu, J., Ma, L.X., Zhang, X.Q., Thomson, J.A., and Zhang, S.C. (2010). Neural differentiation of human induced pluripotent stem cells follows developmental principles but with variable potency. Proc. Natl. Acad. Sci. U S A *107*, 4335–4340.

Hynes, R.O. (2009). The extracellular matrix: not just pretty fibrils. Science *326*, 1216–1219.

Jiang, F.X., Yurke, B., Firestein, B.L., and Langrana, N.A. (2008). Neurite outgrowth on a DNA crosslinked hydrogel with tunable stiffnesses. Ann. Biomed. Eng. *36*, 1565–1579.

Kerstein, P.C., Jacques-Fricke, B.T., Rengifo, J., Mogen, B.J., Williams, J.C., Gottlieb, P.A., Sachs, F., and Gomez, T.M. (2013). Mechanosensitive TRPC1 channels promote calpain proteolysis of talin to regulate spinal axon outgrowth. J. Neurosci. *33*, 273–285.

Kerstein, P.C., Nichol, R.H., and Gomez, T.M. (2015). Mechanochemical regulation of growth cone motility. Front. Cell. Neurosci. *9*, 244.

Kerstein, P.C., Patel, K.M., and Gomez, T.M. (2017). Calpain-mediated proteolysis of talin and FAK regulates adhesion dynamics necessary for axon guidance. J. Neurosci. *37*, 1568–1580.

Koch, D., Rosoff, W.J., Jiang, J., Geller, H.M., and Urbach, J.S. (2012). Strength in the periphery: growth cone biomechanics and substrate rigidity response in peripheral and central nervous system neurons. Biophys. J. *102*, 452–460.

Kohn, J.C., Lampi, M.C., and Reinhart-King, C.A. (2015). Age-related vascular stiffening: causes and consequences. Front. Genet. *6*, 112.

Koser, D.E., Thompson, A.J., Foster, S.K., Dwivedy, A., Pillai, E.K., Sheridan, G.K., Svoboda, H., Viana, M., Costa, L.D., Guck, J., et al. (2016). Mechanosensing is critical for axon growth in the developing brain. Nat. Neurosci. *19*, 1592–1598.

Kostic, A., Sap, J., and Sheetz, M.P. (2007). RPTPalpha is required for rigidity-dependent inhibition of extension and differentiation of hippocampal neurons. J. Cell Sci. *120*, 3895–3904.

Kruse, S.A., Rose, G.H., Glaser, K.J., Manduca, A., Felmlee, J.P., Jack, C.R., Jr., and Ehman, R.L. (2008). Magnetic resonance elastography of the brain. Neuroimage *39*, 231–237.

Kshitiz, Hubbi, M.E., Ahn, E.H., Downey, J., Afzal, J., Kim, D.H., Rey, S., Chang, C., Kundu, A., Semenza, G.L., et al. (2012). Matrix rigidity controls endothelial differentiation and morphogenesis of cardiac precursors. Sci. Signal. *5*, https://doi.org/10.1126/scisignal.2003002.

LaCroix, A.S., Rothenberg, K.E., and Hoffman, B.D. (2015). Molecular-scale tools for studying mechanotransduction. Annu. Rev. Biomed. Eng. *17*, 287–316.

Lawson, C.D., and Burridge, K. (2014). The on-off relationship of Rho and Rac during integrin-mediated adhesion and cell migration. Small GTPases *5*, e27958.

Lessey, E.C., Guilluy, C., and Burridge, K. (2012). From mechanical force to RHOA activation. Biochemistry *51*, 7420–7432.

Lin, C.H., Espreafico, E.M., Mooseker, M.S., and Forscher, P. (1996). Myosin drives retrograde F-actin flow in neuronal growth cones. Neuron *16*, 769–782.

Lin, C.H., and Forscher, P. (1995). Growth cone advance is inversely proportional to retrograde F-actin flow. Neuron *14*, 763–771.

Lowery, L.A., and Van Vactor, D. (2009). The trip of the tip: understanding the growth cone machinery. Nat. Rev. Mol. Cell Biol. *10*, 332–343.

McCracken, P.J., Manduca, A., Felmlee, J., and Ehman, R.L. (2005). Mechanical transient-based magnetic resonance elastography. Magn. Reson. Med. *53*, 628–639.

McKee, C.T., Last, J.A., Russell, P., and Murphy, C.J. (2011). Indentation versus tensile measurements of Young's modulus for soft biological tissues. Tissue Eng. Part B Rev. *17*, 155–164.

Moore, S.W., Roca-Cusachs, P., and Sheetz, M.P. (2010). Stretchy proteins on stretchy substrates: the important elements of integrin-mediated rigidity sensing. Dev. Cell *19*, 194–206.

Moore, S.W., Zhang, X., Lynch, C.D., and Sheetz, M.P. (2012). Netrin-1 attracts axons through FAK-dependent mechanotransduction. J. Neurosci. *32*, 11574–11585.

Morelli, S., Piscioneri, A., Drioli, E., and De Bartolo, L. (2017). Neuronal differentiation modulated by polymeric membrane properties. Cells Tissues Organs *204*, 164–178.

Musah, S., Wrighton, P.J., Zaltsman, Y., Zhong, X., Zorn, S., Parlato, M.B., Hsiao, C., Palecek, S.P., Chang, Q., Murphy, W.L., et al. (2014). Substratum-induced differentiation of human pluripotent stem cells reveals the coactivator YAP is a potent regulator of neuronal specification. Proc. Natl. Acad. Sci. U S A *111*, 13805–13810.

Myers, J.P., and Gomez, T.M. (2011). Focal adhesion kinase promotes integrin adhesion dynamics necessary for chemotropic turning of nerve growth cones. J. Neurosci. *31*, 13585–13595.

Nichol, R.H., Hagen, K.M., Lumbard, D.C., Dent, E.W., and Gomez, T.M. (2016). Guidance of axons by local coupling of retrograde flow to point contact adhesions. J. Neurosci. *36*, 2267–2282.

Oria, R., Wiegand, T., Escribano, J., Elosegui-Artola, A., Uriarte, J.J., Moreno-Pulido, C., Platzman, I., Delcanale, P., Albertazzi, L., Navajas, D., et al. (2017). Force loading explains spatial sensing of ligands by cells. Nature *552*, 219–224.

Paszek, M.J., Zahir, N., Johnson, K.R., Lakins, J.N., Rozenberg, G.I., Gefen, A., Reinhart-King, C.A., Margulies, S.S., Dembo, M., Boettiger, D., et al. (2005). Tensional homeostasis and the malignant phenotype. Cancer Cell *8*, 241–254.

Robles, E., and Gomez, T.M. (2006). Focal adhesion kinase signaling at sites of integrin-mediated adhesion controls axon pathfinding. Nat. Neurosci. *9*, 1274–1283.

Roeder, B.A., Kokini, K., Sturgis, J.E., Robinson, J.P., and Voytik-Harbin, S.L. (2002). Tensile mechanical properties of three-dimensional type I collagen extracellular matrices with varied microstructure. J. Biomech. Eng. *124*, 214–222.

Sahai, E., and Olson, M.F. (2006). Purification of TAT-C3 exoenzyme. Methods Enzymol. *406*, 128–140.

Sawada, Y., Tamada, M., Dubin-Thaler, B.J., Cherniavskaya, O., Sakai, R., Tanaka, S., and Sheetz, M.P. (2006). Force sensing by mechanical extension of the SRC family kinase substrate p130Cas. Cell *127*, 1015–1026.

Schiller, H.B., and Fassler, R. (2013). Mechanosensitivity and compositional dynamics of cell-matrix adhesions. EMBO Rep. *14*, 509–519.

Shimizu, Y., Boehm, H., Yamaguchi, K., Spatz, J.P., and Nakanishi, J. (2014). A photoactivatable nanopatterned substrate for analyzing collective cell migration with precisely tuned cell-extracellular matrix ligand interactions. PLoS One *9*, e91875.

Sholl, A., and Uttley, A.M. (1953). Pattern discrimination and the visual cortex. Nature *171*, 387–388.

Stankiewicz, T.R., and Linseman, D.A. (2014). Rho family GTPases: key players in neuronal development, neuronal survival, and neurodegeneration. Front. Cell. Neurosci. *8*, 314.

Sun, Z., Guo, S.S., and Fassler, R. (2016). Integrin-mediated mechanotransduction. J. Cell Biol. *215*, 445–456.

Sundararaghavan, H.G., Monteiro, G.A., Firestein, B.L., and Shreiber, D.I. (2009). Neurite growth in 3D collagen gels with gradients of mechanical properties. Biotechnol. Bioeng. *102*, 632–643.

Sundararaghavan, H.G., Monteiro, G.A., Lapin, N.A., Chabal, Y.J., Miksan, J.R., and Shreiber, D.I. (2008). Genipin-induced changes in collagen gels: correlation of mechanical properties to fluorescence. J. Biomed. Mater. Res. A *87*, 308–320.

Tessier-Lavigne, M., and Goodman, C.S. (1996). The molecular biology of axon guidance. Science *274*, 1123–1133.

Tyler, W.J. (2012). The mechanobiology of brain function. Nat. Rev. Neurosci. *13*, 867–878.

Vicente-Manzanares, M., Choi, C.K., and Horwitz, A.R. (2009). Integrins in cell migration—the actin connection. J. Cell Sci. *122*, 199–206.

Wang, Y., Botvinick, E.L., Zhao, Y., Berns, M.W., Usami, S., Tsien, R.Y., and Chien, S. (2005). Visualizing the mechanical activation of SRC. Nature *434*, 1040–1045.

Willits, R.K., and Skornia, S.L. (2004). Effect of collagen gel stiffness on neurite extension. J. Biomater. Sci. Polym. Ed. *15*, 1521–1531.

Woo, S., and Gomez, T.M. (2006). Rac1 and RHOA promote neurite outgrowth through formation and stabilization of growth cone point contacts. J. Neurosci. *26*, 1418–1428.

Woo, S., Rowan, D.J., and Gomez, T.M. (2009). Retinotopic mapping requires focal adhesion kinase-mediated regulation of growth cone adhesion. J. Neurosci. *29*, 13981–13991.

Yunoki, S., Ohyabu, Y., and Hatayama, H. (2013). Temperature-responsive gelation of type I collagen solutions involving fibril formation and genipin crosslinking as a potential injectable hydrogel. Int J Biomater.